



Fig. S1 Optical images of one MORB (black) and seven CMAS glasses equilibrated in (a,b) wells drilled in 25 mm diameter Al_2O_3 disks at **(a)** 1 atmosphere, 1300 °C, and $\log f\text{O}_2 = -1$ ($\Delta\text{QFM} = 7.3$), **(b)** 1 atmosphere, 1300 °C, and $\log f\text{O}_2 = -7$ ($\Delta\text{QFM} = 0.3$), and **(c)** Pt capsules at 1.0 GPa, 1400 °C and $\log f\text{O}_2 = 4.8$ ($\Delta\text{QFM} = 11$), mounted and sectioned in epoxy.

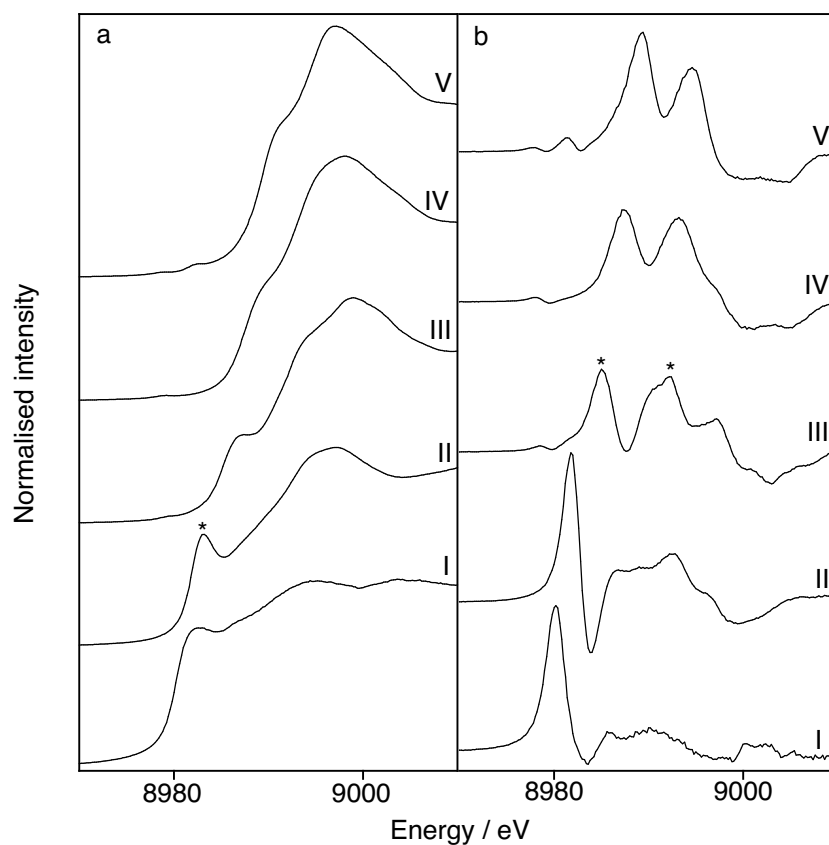


Fig. S2 (a) Cu *K*-edge XANES spectra of standard compounds and **(b)** the corresponding derivative spectra of (I) Cu⁰ metal, (II) Cu⁺₂O, (III) Cu²⁺O, (IV) Cu(NO₃)₂·3H₂O and (V) CuSO₄·5H₂O. The 1*s*→4*p* peak of Cu⁺ in (a) and the shoulder (α) and main edge (β) of Cu²⁺ in (b) are indicated by *.

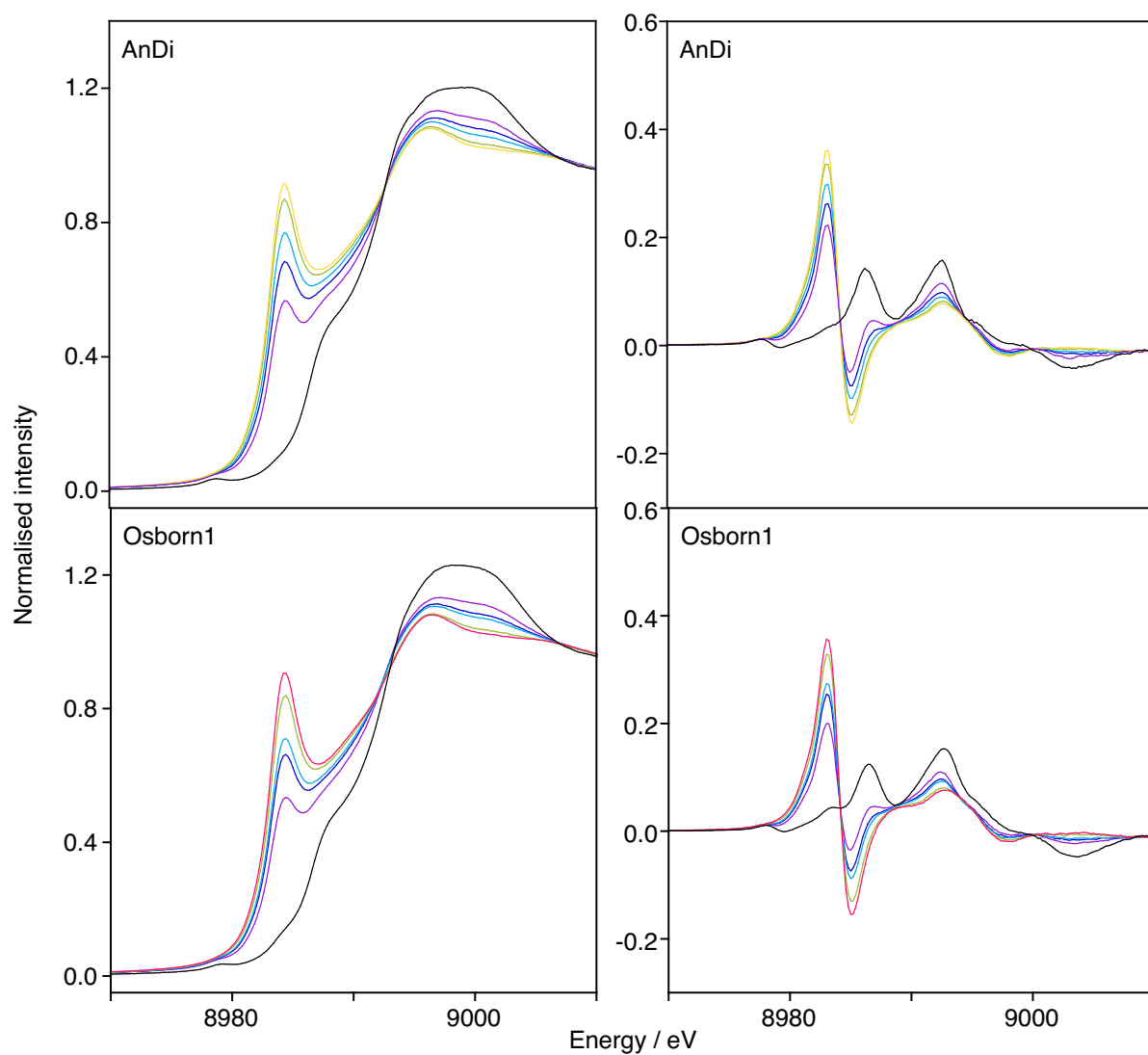


Fig. S3 Cu *K*-edge XANES spectra and the corresponding derivative spectra, recorded at the AS, of AnDi, Osborn1, Osborn3, Osborn4, Osborn6, CAS1, CAS4, CAS5, Longhi2, Longhi3, Longhi4, Na1, Na2, Na3, Na4, Na5, Na6 redox series glasses quenched from melts equilibrated at 1.0 GPa, 1400 °C and $\log f\text{O}_2 = 4.7$ (black) and 1 atm, 1300 °C and $\log f\text{O}_2 = 0$ (purple), -1 (dark blue), -2 (light blue), -3 (green), -5 (yellow), -6 (orange), -7 (pink) and -8 (red). Anomalous spectra are shown using dashed lines.

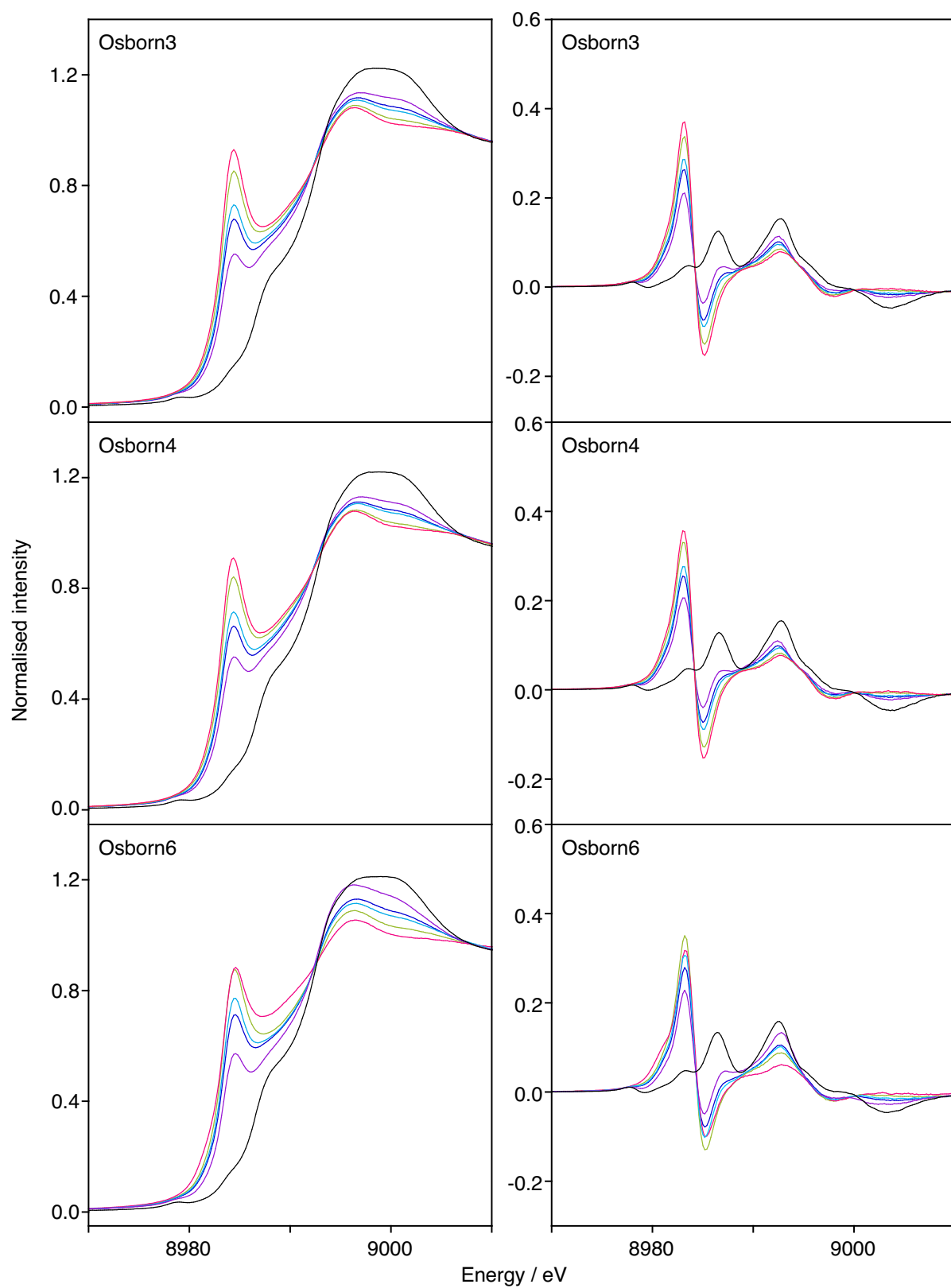


Fig. S3 cont.

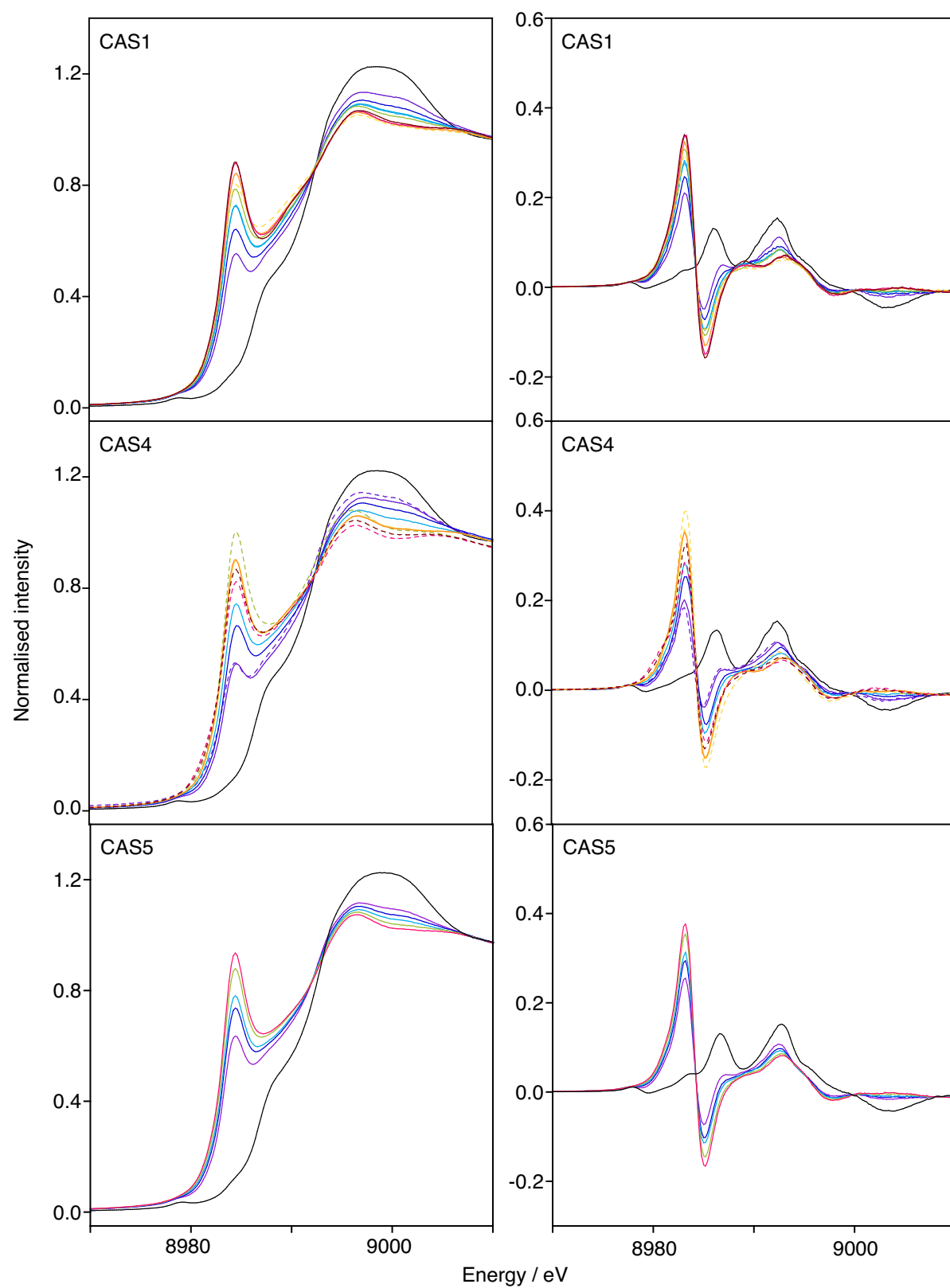


Fig. S3 cont.

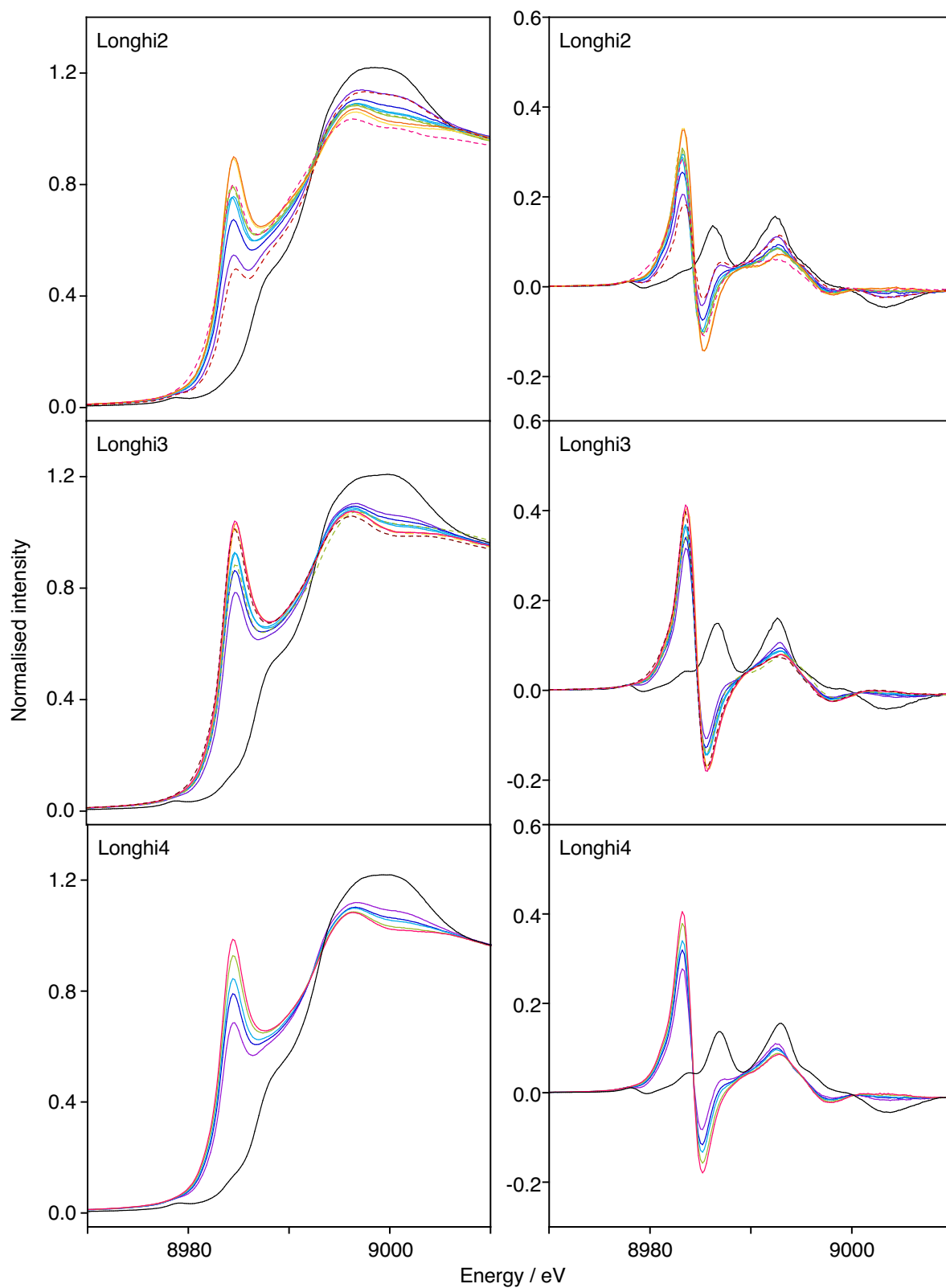


Fig. S3 cont.

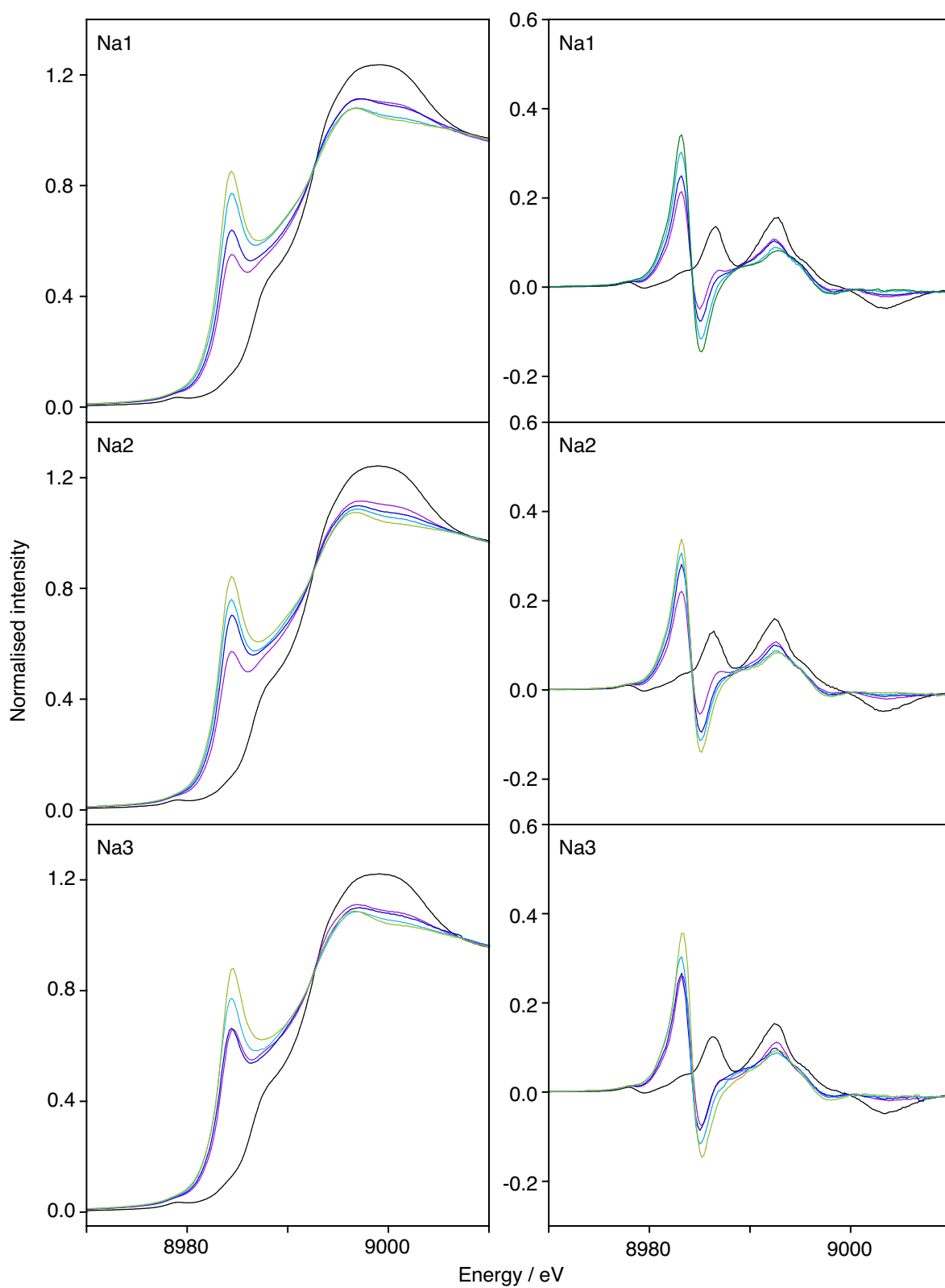


Fig. S3 cont.

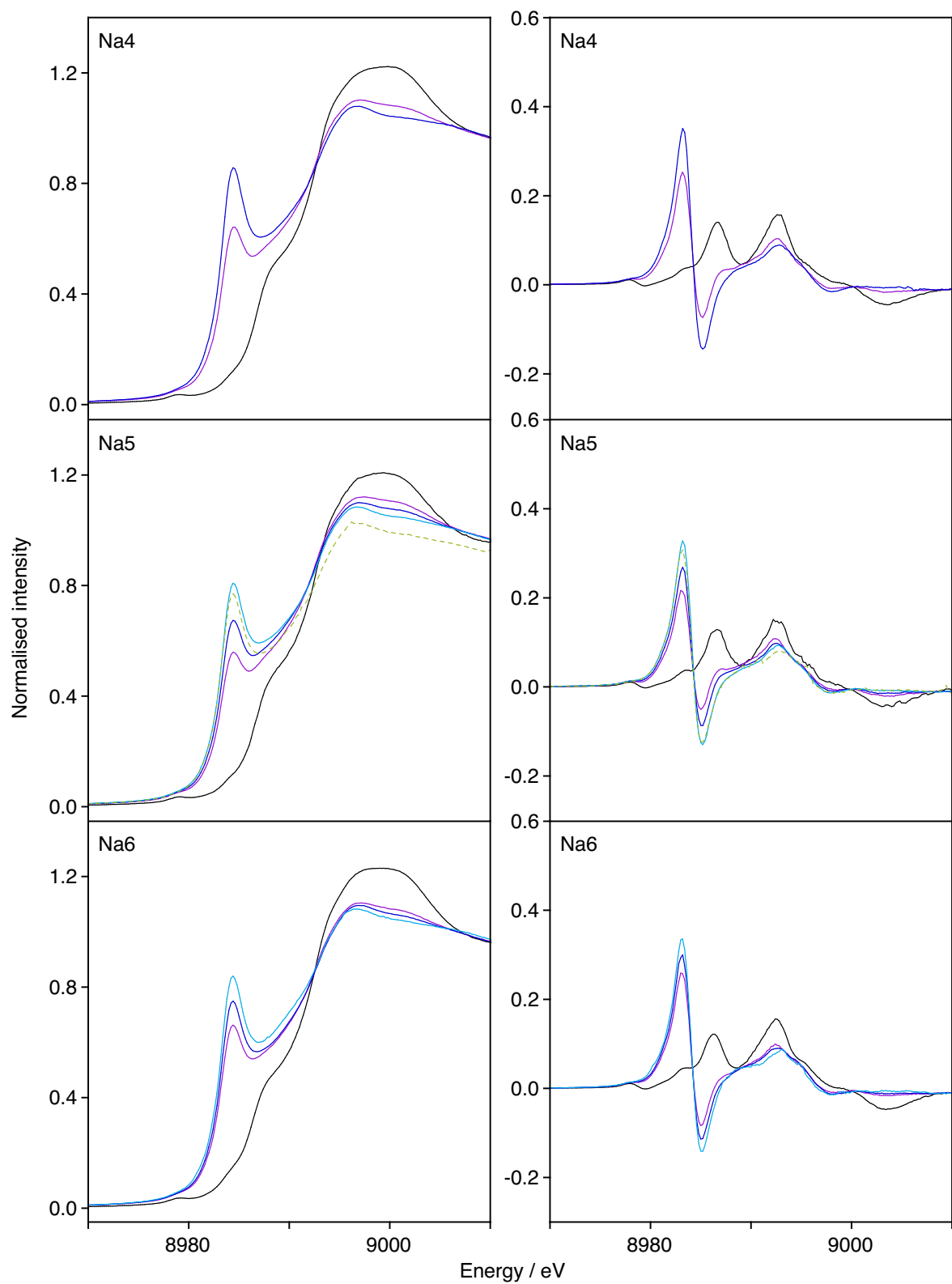


Fig. S3 cont.

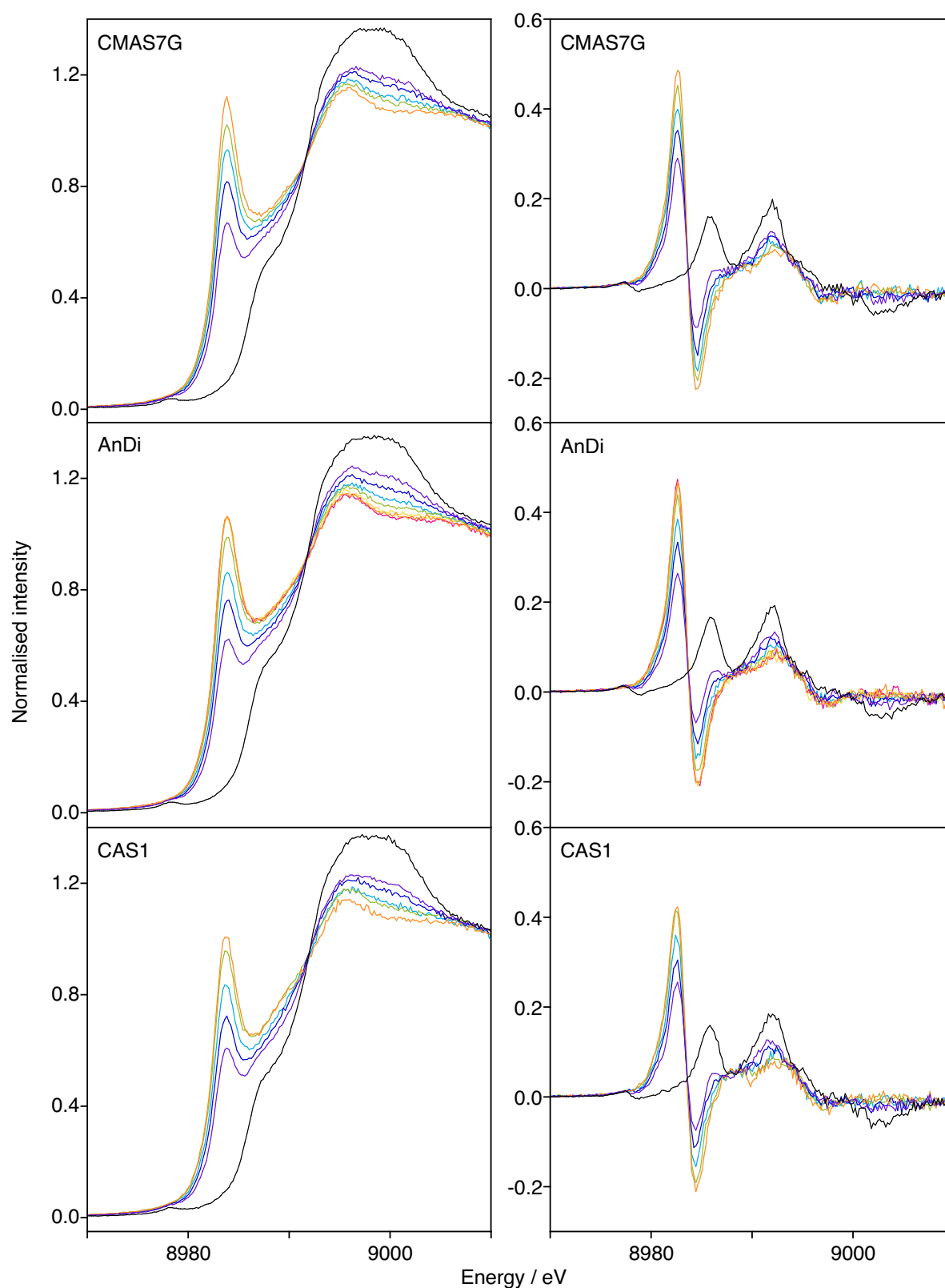


Fig. S4 Cu *K*-edge XANES spectra and the corresponding derivative spectra, recorded at the APS, of CMAS7G, AnDi, CAS1, CAS4, Longhi2 and Longhi3 redox series glasses quenched from melts equilibrated at 1.0 GPa, 1400 °C and $\log f_{\text{O}_2} = 4.7$ (black) and 1 atm, 1300 °C and $\log f_{\text{O}_2} = 0$ (purple), -1 (dark blue), -2 (light blue), -3 (green), -5 (yellow), -6 (orange), -7 (pink) and -8 (red).

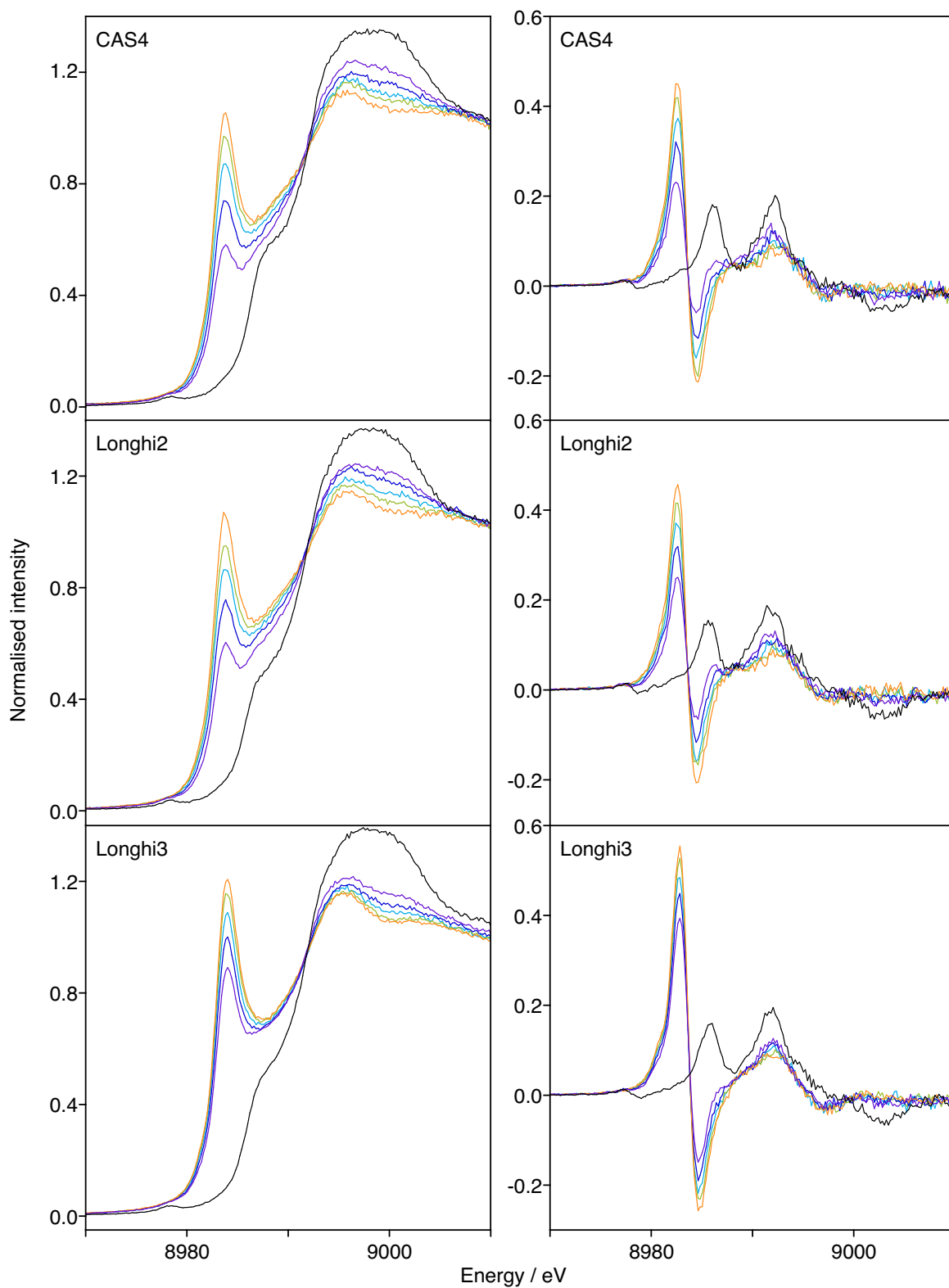


Fig. S4 cont.

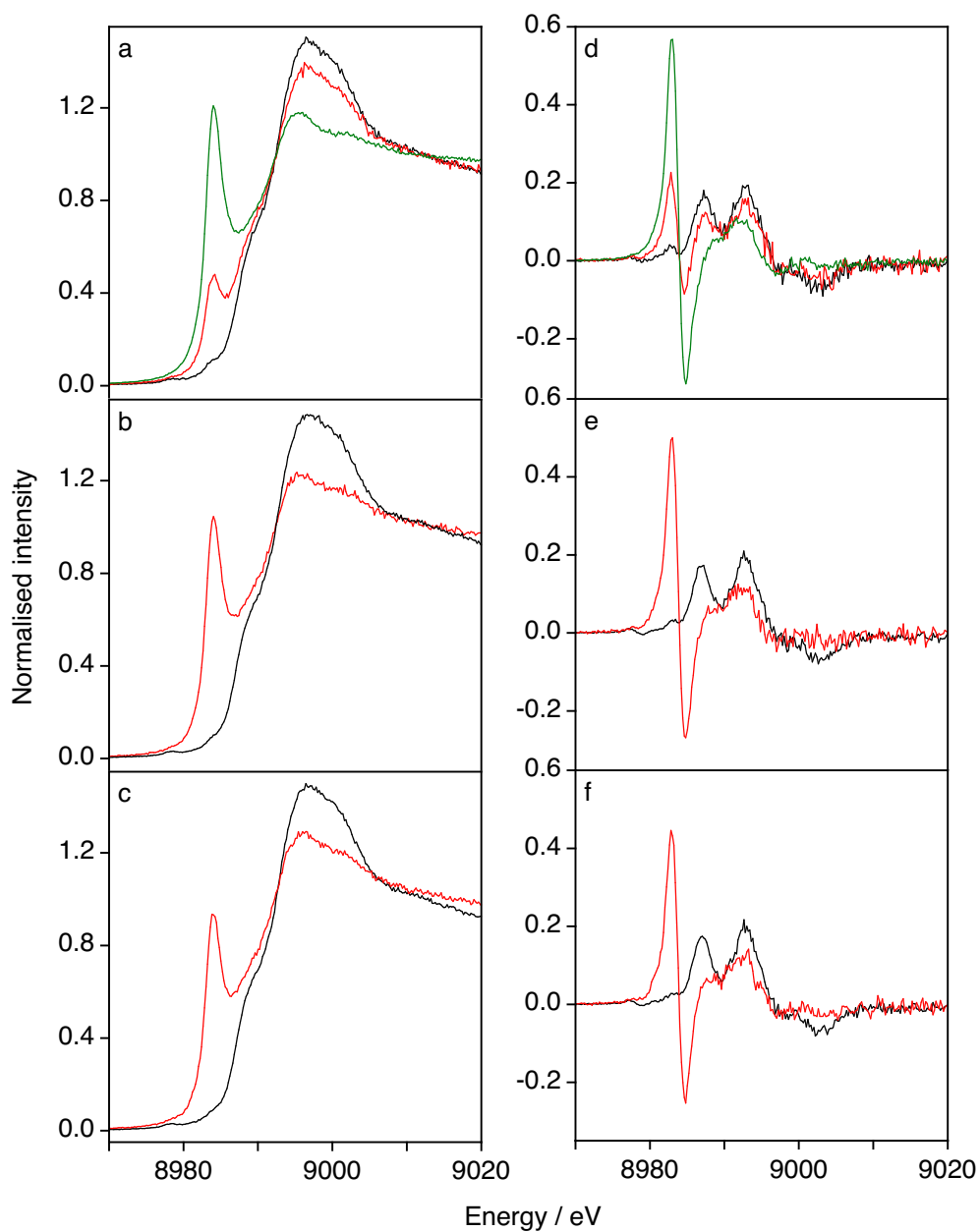


Fig. S5 Cu *K*-edge XANES spectra recorded at the APS and the corresponding derivative spectra of hydrous granite glasses quenched from melts equilibrated at **(a, d)** 900, **(b, e)** 1100 and **(c, f)** 1400 °C, 1 GPa and with Pt-PtO₂ (black), Ru-RuO₂ (red) and Cu-Cu₂O (green).

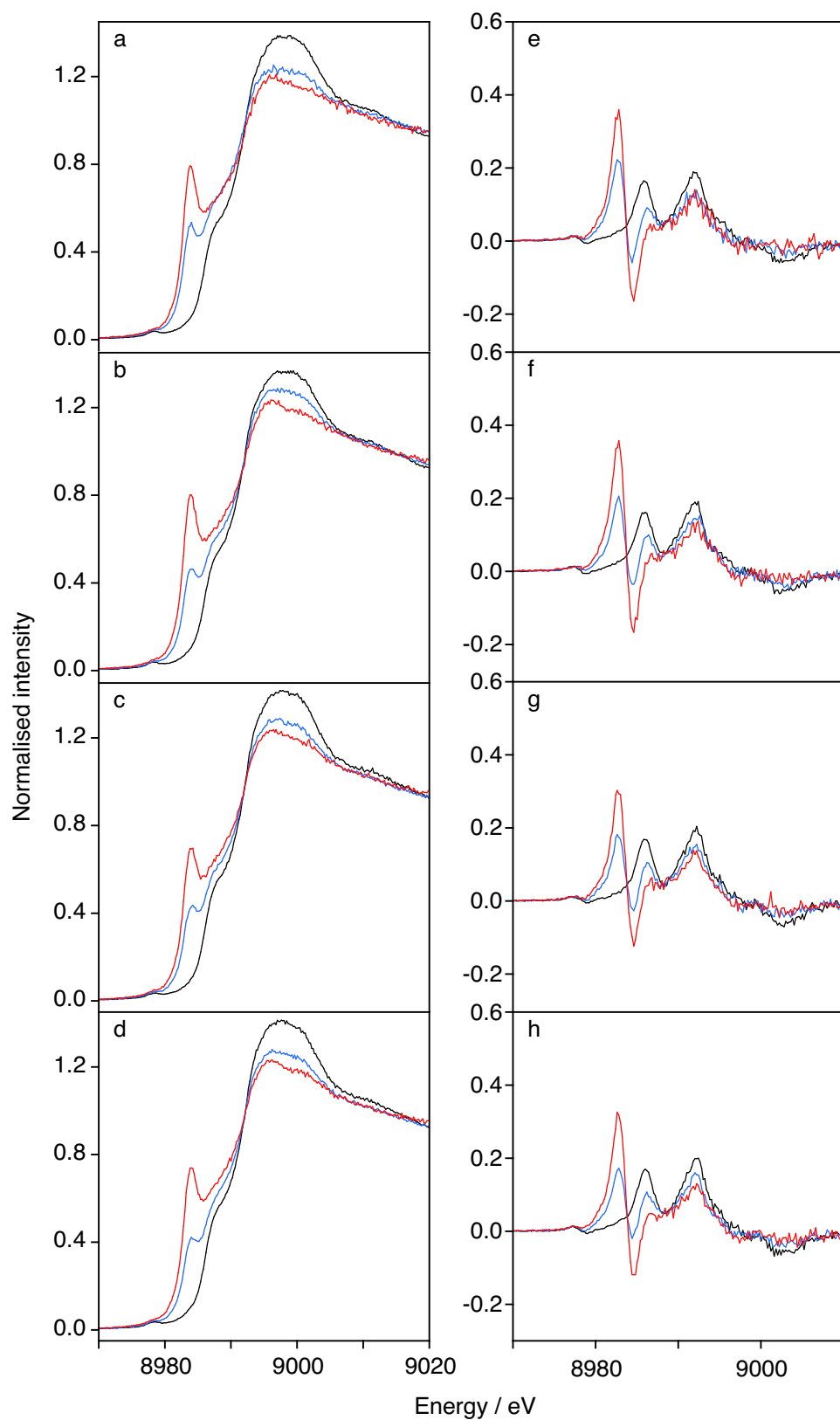


Fig. S6 Cu *K*-edge XANES spectra recorded at the APS and the corresponding derivative spectra of CMAS7G glasses quenched from melts equilibrated at **(a, e)** 0.5, **(b, f)** 1.0, **(c, g)** 2.0, **(d, h)** 2.5 GPa, 1400 °C and with PtO₂ (black), Ir-IrO₂ (blue) and Ru-RuO₂ (red).

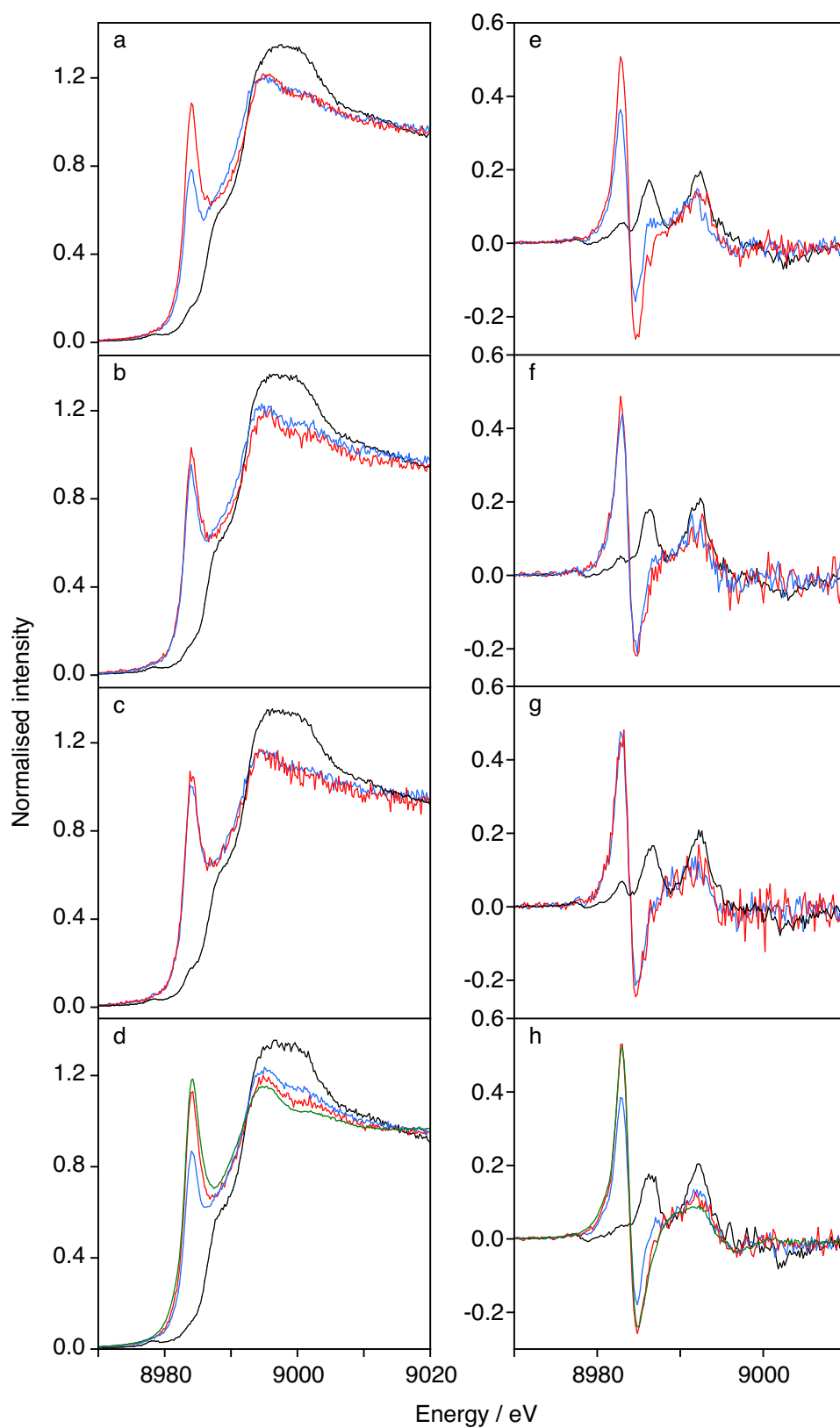


Fig. S7 Cu *K*-edge XANES spectra recorded at the APS and the corresponding derivative spectra of granite glasses quenched from melts equilibrated at (a, e) 0.5, (b, f) 1.0, (c, g) 2.0, (d, h) 2.5 GPa, 1400 °C and with Pt-PtO₂ (black), Ir-IrO₂ (blue), Ru-RuO₂ (red) and Re-ReO₂ (green).

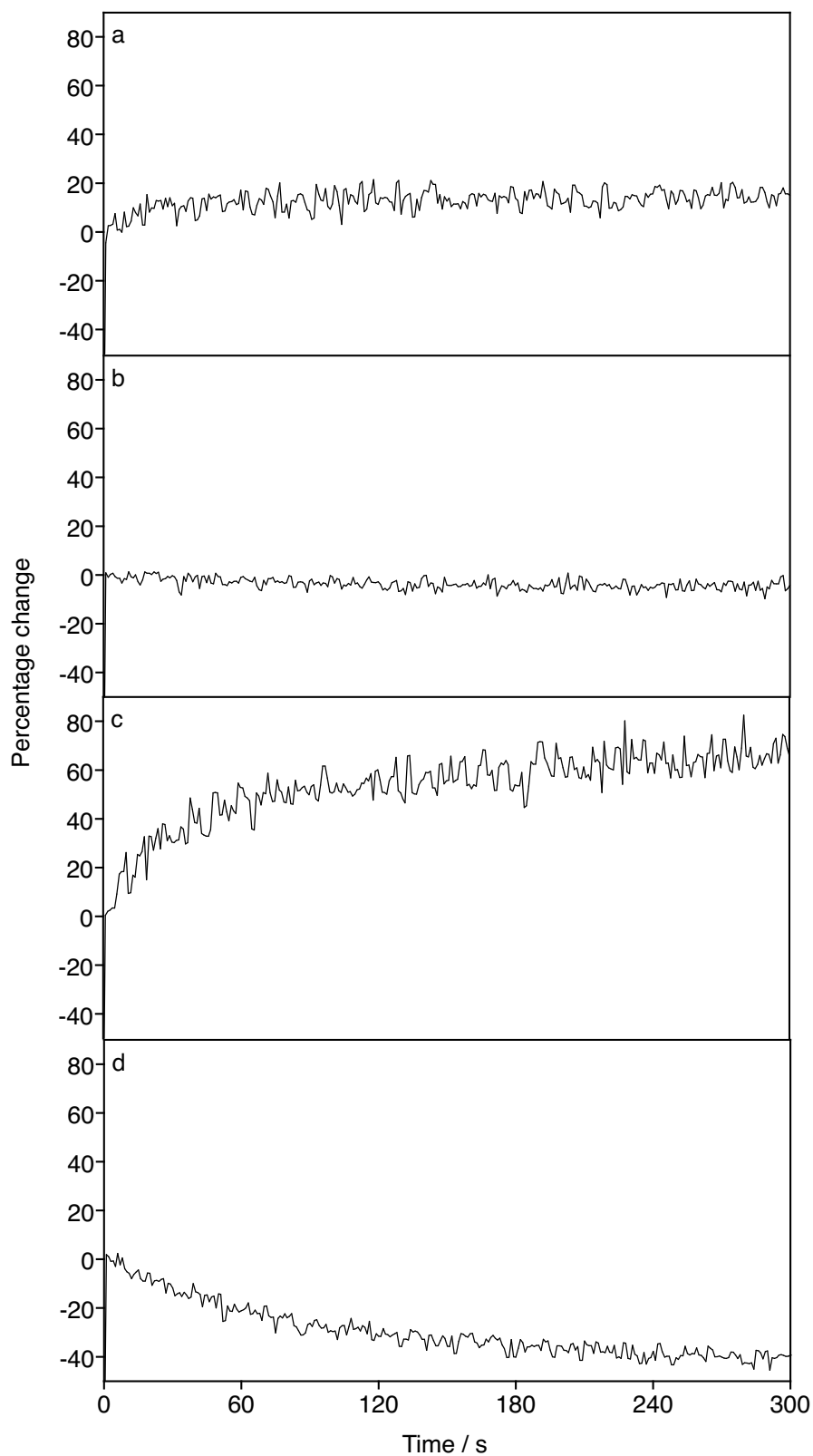


Fig. S8 Percentage change in the I_0 normalised fluorescence intensity at the energy of the $1s \rightarrow 4p$ peak (~ 8984 eV) as a function of time for **(a, b)** CMAS7G glasses quenched from melts equilibrated at 1400°C , 2.5 GPa and **(a)** $\Delta\text{FMQ} = 11$ and **(b)** $\Delta\text{FMQ} = 5.1$, and **(c, d)** hydrous granite equilibrated at 1400°C , 1.0 GPa and **(c)** $\Delta\text{FMQ} = 10.6$ and **(d)** $\Delta\text{FMQ} = 6.5$.

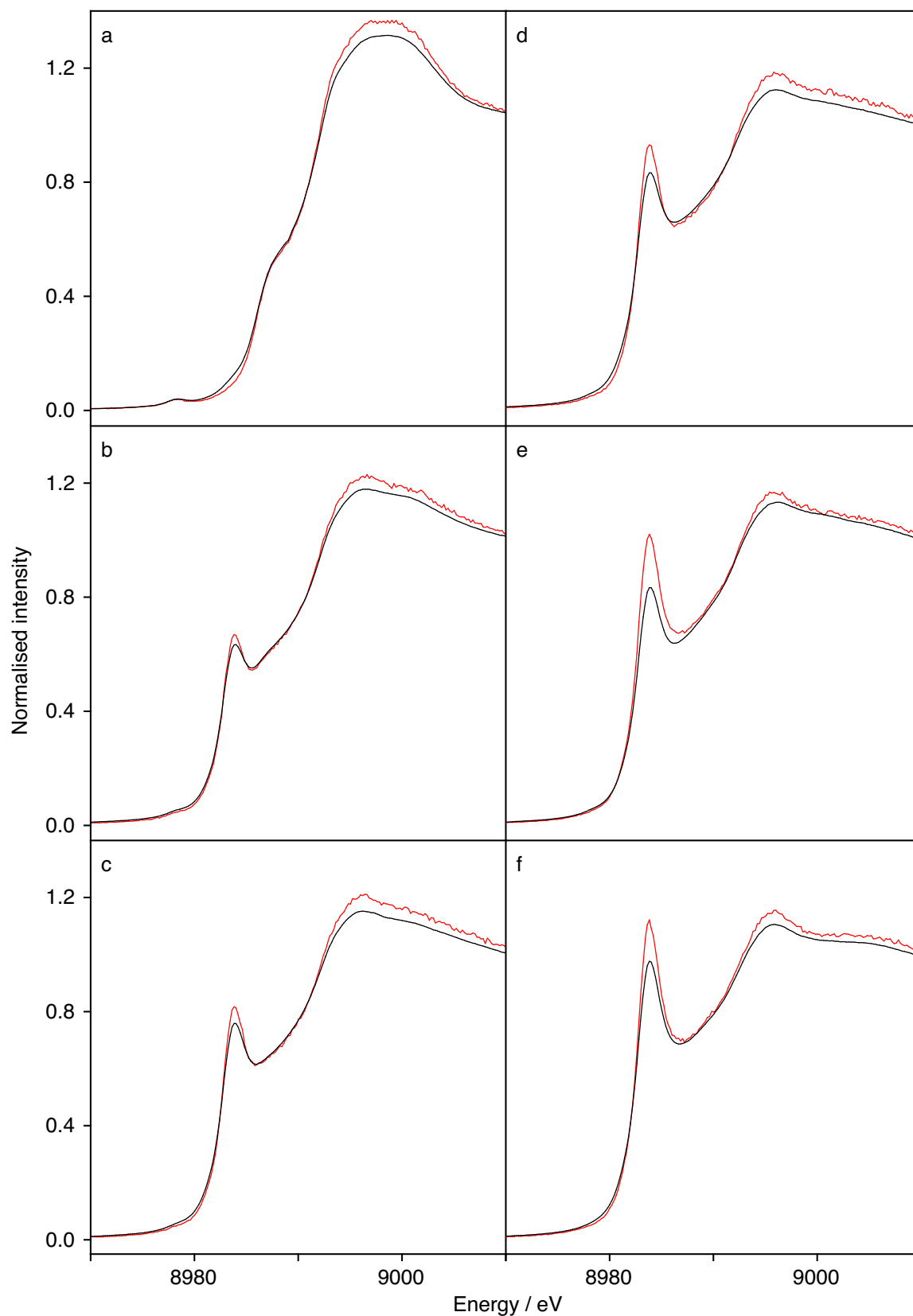


Fig. S9 Cu *K*-edge XANES spectra recorded at the APS (red) and AS (black) from CMAS7G glasses quenched from melts equilibrated at **(a)** 1.0 GPa, 1400 °C and $\log f_{\text{O}_2} = 4.7$ (black), and 1 atm, 1300 °C and $\log f_{\text{O}_2} =$ **(b)** 0, **(c)** -1, **(d)** -2, **(e)** -3, and **(f)** -6.

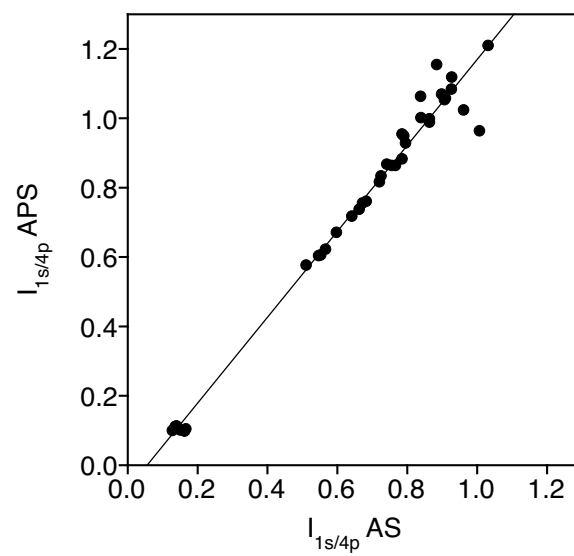


Fig. S10 $I_{1s/4p}$ of spectra recorded from glasses at both the APS and AS. The line of best fit is shown.

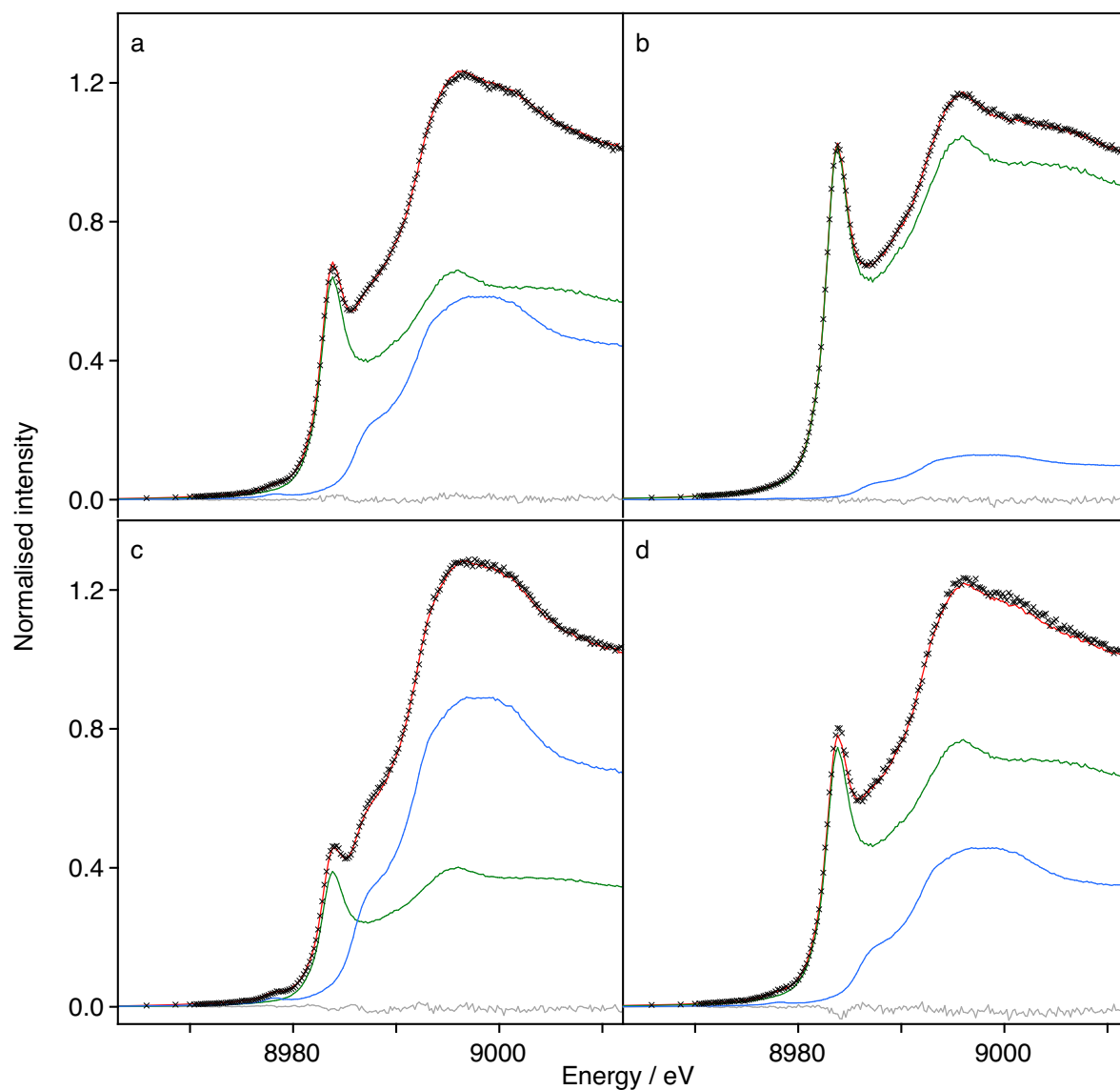


Fig. S11 Linear combination fits of Cu *K*-edge XANES spectra of CMAS7G glasses quenched from melts equilibrated at 1atm, 1300 °C and $\log f_{\text{O}_2}$ = **(a)** 0 and **(b)** -3, and 1.0 GPa, 1400 °C with **(c)** Ir-IrO₂ and **(d)** Ru-RuO₂. The data are denoted by the symbols, and the fit (red), residual (grey), Cu²⁺ end-member (CMAS7G equilibrated at ΔFMQ = 11, 1.0 GPa and 1400 °C; blue) and Cu⁺ end-member (CMAS7G equilibrated at ΔFMQ = -7, 1.0 GPa and 1400 °C; green) by the solid lines. The fit range is shown.

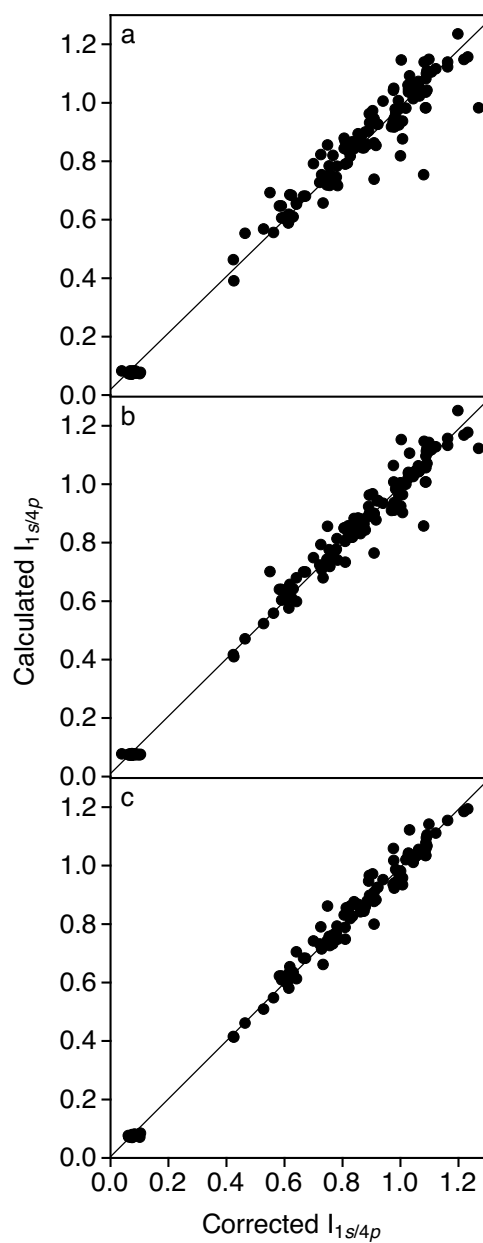


Fig. S12 $I_{1s/4p}$ calculated by fitting the corrected $I_{1s/4p}$ to Eq. 8 with composition parameterised by **(a)** NBO/T, **(b)** optical basicity and **(c)** single cation mole fractions versus the corrected $I_{1s/4p}$ (Table 2 and 3). The lines are the best fits to the data.

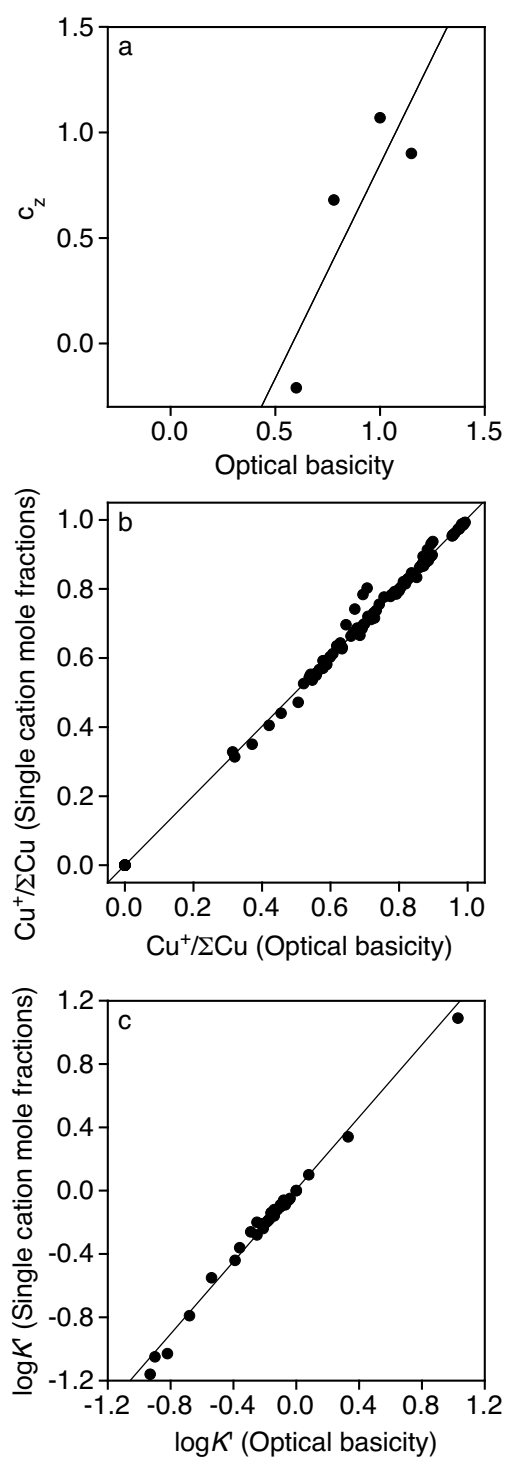


Fig. S13 (a) Correlation between c_z parameters and optical basicity coefficients of Al_2O_3 , MgO , CaO and Na_2O , (b) $\text{Cu}^+/\Sigma\text{Cu}$ and (c) $\log K'$ determined from fitting Eq. 8 with melt composition parameterised by single cation mole fractions versus those determined with melt composition parameterised by optical basicity. The lines are the best fits to the data.